

Asymmetric Photocross-Linking of Singly Phosphorylated Smooth Muscle Heavy Meromyosin

Kosuke Takeya¹, Masayuki Takahashi¹, Tsuyoshi Katoh² and Michio Yazawa^{1,*}

¹Division of Chemistry, Graduate School of Science, Hokkaido University, Sapporo 060-0810; and ²Department of Biochemistry, Asahikawa Medical College, Asahikawa 078-8510

Received April 27, 2005; accepted May 29, 2005

Although activities of smooth muscle myosin are regulated by phosphorylation, the molecular mechanisms of regulation have not been fully established. Phosphorylation of both heads of myosin is known to activate ATPase and motor activities, but the effects of phosphorylation of only one of the heads have not been established. Such information on singly phosphorylated myosin can serve to elucidate the molecular mechanism of the phosphorylation-dependent regulation. To understand the structural properties of the singly phosphorylated state, we prepared singly phosphorylated heavy meromyosin (HMM) containing a photoreactive benzophenone-labeled RLC and examined its photocross-linking reactivity. The two heads in the singly phosphorylated HMM showed different reactivities. The dephosphorylated RLC in the singly phosphorylated HMM was cross-linked to a heavy chain, like that in the dephosphorylated HMM, whereas the phosphorylated RLC did not react, like that in the fully phosphorylated HMM. These results indicate that the two heads of the singly phosphorylated HMM have an asymmetric structure, suggesting that phosphorylation of one head can to some extent activate smooth muscle HMM.

Key words: benzophenone, heavy meromyosin, photocross-linking, phosphorylation, smooth muscle myosin.

Abbreviations: 1P-HMM, singly (thio)phosphorylated HMM; BPIA, benzophenone-4-iodoacetamide; BP-HMM, HMM exchanged with BP-RLC; BP-RLC, benzophenone-labeled RLC; ELC, essential light chain; HC, myosin heavy chain; HMM, heavy meromyosin; MOPS, 3-(*N*-morpholino)propanesulfonic acid; PMSF, phenylmethylsulfonyl fluoride; RLC, regulatory light chain.

Smooth muscle myosin is a motor protein which moves actin filaments. Smooth muscle myosin is composed of two globular head domains and a rod-like tail domain. Each head has a motor domain containing one actin-binding and one nucleotide-binding site. The motor activity of smooth muscle myosin is regulated by phosphorylation of the regulatory light chain (RLC), which binds to the C-terminus of the head (regulatory domain) with the essential light chain (ELC) (1–4). Dephosphorylated myosin has a low actin-activated MgATPase activity and does not move actin filaments. Phosphorylation of Ser19 on the RLC dramatically increases the actin-activated MgATPase activity and thereby initiates actin movement.

How is the phosphorylation event on the RLC transmitted to the motor domain? Removal of the RLC results in activation of the actin-activated MgATPase activity compared to the dephosphorylated myosin (5, 6). In contrast, the activity of myosin lacking the ELC is substantially inhibited in the dephosphorylated state, and activated by phosphorylation of the RLC (5, 6). These results clearly indicate that the RLC is essential for the inhibition in the dephosphorylated state. A monomeric head domain, myosin subfragment 1 (7–9), or a single-headed myosin (10, 11) has a motor activity even in the dephosphorylated state. On the other hand, a double-headed

myosin subfragment, heavy meromyosin (HMM), shows complete regulation by phosphorylation (8, 9), suggesting that the double-headed structure is required for the phosphorylation-dependent regulation. Recent studies on a series of single-headed HMMs (12–14) support this notion and provide a new idea that two heads are required for phosphorylation-dependent release from inhibitory interactions between a head and the S2 region.

Whether phosphorylation of one head affects the inhibitory interaction is also an important question related to the regulatory mechanism. The singly phosphorylated myosin is in an intermediate state of phosphorylation, with one head phosphorylated and the other dephosphorylated. Clarifying how the phosphorylated and the dephosphorylated heads affect each other in the singly phosphorylated state will elucidate the mechanisms of activation by phosphorylation. However, properties of the singly phosphorylated myosin have not been established yet. Harris *et al.* (15) reported that the activation of the phosphorylated head was independent of the dephosphorylated partner head in singly phosphorylated myosin. In contrast, Ellison *et al.* (16) showed that both heads were partially activated in singly phosphorylated HMM (1P-HMM).

In this study, we examined structural properties of 1P-HMM and discussed the effects of phosphorylation on the interactions between the two head domains. It was reported that chemical cross-linking reactivity of HMM was affected by phosphorylation of both heads, suggest-

*To whom correspondence should be addressed. Tel: +81-11-706-3813, Fax: +81-11-706-4924, E-mail: myazawa@sci.hokudai.ac.jp

ing that the spatial relationship of the two heads was altered by phosphorylation (17). According to this report, we prepared 1P-HMMs in which one of the two RLCs, either the phosphorylated or the dephosphorylated one, was labeled with a photoreactive benzophenone (BP) reagent and examined their cross-linking reactivities. The BP-label showed different reactivities in each 1P-HMM depending on whether it is on the dephosphorylated or phosphorylated RLC. This result demonstrated the asymmetric nature of the two heads in the singly phosphorylated state.

MATERIALS AND METHODS

Protein Preparations—HMM was prepared by digesting chicken gizzard smooth muscle myosin (18) with *Staphylococcus aureus* V8 protease (8). Actin was obtained from rabbit skeletal muscle (19). Myosin light chain kinase (20) and calmodulin (21) were obtained from chicken gizzard smooth muscle. The concentrations of HMM, actin and calmodulin were determined from the absorbance at 280 nm using the absorbance coefficients of 0.65, 1.10 and 0.21 (mg/ml)⁻¹ cm⁻¹, respectively. The concentrations of myosin light chain kinase and recombinant RLC were determined by the biuret method using bovine serum albumin as a standard (22).

Purification of Expressed RLC—His-tag fused RLC (His-RLC) was expressed in *Escherichia coli*. The cDNA for chicken smooth muscle myosin regulatory light chain was inserted into the *NspV* and *EcoRI* sites of the expression vector pET-30b(+) generating pET-RLC. *E. coli* BL21 (DE3) was transformed with pET-RLC. The RLC expression was induced by adding 0.1 mM isopropyl-1-thio-β-D-galactopyranoside when the absorbance at 600 nm reached 1.0. The cells were grown overnight at 37°C and harvested by centrifugation at 4,800 × *g* for 15 min. The cells were suspended in lysis solution (8 M urea, 0.5 M NaCl, 10 mM imidazole, 1 mM benzamidine, 1 mM PMSF, 50 mM sodium phosphate, pH 7.0) and stirred at room temperature for 1 h. After centrifugation at 36,000 × *g* for 30 min, the supernatant was loaded onto a Ni²⁺-Chelating Sepharose Fast Flow (Amersham Biosciences) column (2.2 × 5 cm) that had been equilibrated with binding solution (8 M urea, 0.5 M NaCl, 10 mM imidazole, 50 mM sodium phosphate, pH 7.0). The column was washed with 5 volumes of 50 mM imidazole in the binding solution. His-RLC was eluted with 5 volumes of 300 mM imidazole in the binding solution. The fractions containing His-RLC were dialyzed against 50 mM ammonium bicarbonate, 1 mM DTT at 4°C to remove urea. The insol-

uble fraction was removed by centrifugation at 36,000 × *g* for 30 min. His-RLC was lyophilized and stored at -20°C. The expressed RLC has a 27-amino acid extension MHH-HHHHSSGLVPRGSGMKETAALKFE at the N-terminus of the native protein sequence (SSK...KDD).

Labeling of RLC with BPIA—His-RLC was labeled with benzophenone-4-iodoacetamide (BPIA) (Molecular Probes) at the single cysteine residue (Cys108) according to previous reports (17, 23) with a few modifications. The lyophilized RLC was dissolved in 50 mM ammonium bicarbonate, 0.1 mM EGTA and 0.1 mM EDTA. DTT was added to 10 mM, and the sample was incubated at 30°C for 1 h to reduce RLC. The reduced RLC (2–3 mg/ml) was dialyzed against the same solution without DTT until the DTT concentration decreased to approximately one-half of the protein concentration. A 1.5-fold molar excess of BPIA over total thiol groups was added, and the sample was stirred at room temperature for 1 h in the dark. The reaction was stopped by adding DTT to 0.5 mM. Unreacted BPIA was removed by gel filtration through a Sephadex G-50 Superfine column. The extent of labeling was estimated spectrophotometrically with the absorbance at 302 nm using the molar extinction coefficient of 22,500 M⁻¹ cm⁻¹ for the BP-RLC (17, 23). Under the conditions described above, 87–95% of RLC was labeled with BPIA.

Exchange of Endogenous RLC with Labeled RLC and Photocross-Linking—BP-labeled RLC was introduced into HMM by exchange with endogenous RLC as described previously (16, 17). HMM was incubated with a 2- to 20-fold molar excess of the labeled RLC in 20 mM sodium phosphate (pH 7.5), 0.5 M NaCl, 10 mM EDTA, 2 mM EGTA, 2 mM ATP and 5 mM DTT at 42°C for 30 min. The sample was allowed to stand at room temperature for 10 min before adding MgCl₂ to 20 mM, then placed on ice. Free RLC was removed by gel filtration through a Sephacryl S-300 HR column (2.6 × 50 cm). Singly exchanged HMM with a single exogenous and a single endogenous RLC was prepared as described previously (16) with a few modifications. Dephosphorylated BP-RLC (BPdp-RLC) was introduced into thiophosphorylated HMM (2P-HMM), yielding a mixture of three species: unexchanged 2P-HMM, singly exchanged 1P-HMM with BPdp-RLC [termed 1P-HMM (BPdp)], and doubly exchanged 0P-HMM with two BPdp-RLCs. In the same way, introduction of thiophosphorylated BP-RLC (BPtp-RLC) into dephosphorylated HMM (0P-HMM) generated a mixture of unexchanged 0P-HMM, singly exchanged 1P-HMM with BPtp-RLC [termed 1P-HMM (BPtp)], and doubly exchanged 2P-HMM with two BPtp-RLCs. After

Table 1. Compositions of HMMs used in this study.

| No. | HMM | RLC used for exchange | Peak of Ni ²⁺ -affinity chromatography | | |
|-----|--------|-----------------------|---|---|-----------------------|
| | | | 1st | 2nd | 3rd |
| (1) | 2P-HMM | BPdp-RLC | 2P-HMM (0 BPdp-RLC) | 1P-HMM* (1 BPdp-RLC) | 0P-HMM* (2 BPdp-RLCs) |
| (2) | 0P-HMM | BPtp-RLC | 0P-HMM (0 BPtp-RLC) | 1P-HMM* (1 BPtp-RLC) | 2P-HMM* (2 BPtp-RLCs) |
| (3) | 0P-HMM | BPdp-RLC | without Ni ²⁺ -affinity chromatography | 0P-HMM* (mixture of 0, 1, and 2 BPdp-RLC) | |

A series of BP-HMMs in various phosphorylation states were prepared by partial exchange between HMM and BP-RLC. Unexchanged, and singly and doubly exchanged HMMs were separated by Ni²⁺-affinity chromatography in (1) and (2). For comparison with the previous report of photocross-linking (17) and assessment of the effects of exposure to non-reducing conditions and Ni²⁺, dephosphorylated BP-HMM (containing 50–60% BPdp-RLC) was obtained without Ni²⁺-affinity chromatography in (3). HMM preparations marked with an asterisk and 2P-HMM (2 BPtp-RLC) prepared by thiophosphorylation of 0P-HMM* of (3) with MLCK were employed for experiments in this study. Unexchanged RLC is unlabeled, so that the RLC is silent in the cross-linking experiments.

gel filtration, the exchanged mixtures of HMM were immediately applied to a 5-ml Ni²⁺-HiTrap chelating column (Amersham Biosciences) in 10 mM MOPS (pH 8.0), 0.3 M NaCl. Elution with a linear gradient of 0–0.3 M imidazole (50 column volumes) separated the three HMM species. Eluate was collected in fractions of 3 ml/tube, and DTT was immediately added into each tube to 2 mM. After SDS-PAGE analysis, fractions containing singly or doubly exchanged HMM were combined and HMM was precipitated by adding 2 volumes of saturated ammonium sulfate solution (pH 7.0). The precipitated HMM was dissolved in 10 mM MOPS (pH 7.5), 0.1 mM EGTA, and 1 mM DTT, and dialyzed against the same solution for 2 h. Thrombin (1 unit/mg HMM) was then added to the sample, and dialysis was continued overnight. Removal of His-tags was confirmed by SDS-PAGE. After extensive dialysis, BP-labeled HMM was ultracentrifuged at 520,000 × *g* for 15 min, and the supernatant was filtered through a 0.45- μ m cellulose acetate filter (Toyo). Photocross-linking was carried out as follows: immediately after addition of fresh DTT to 1 mM, BP-labeled HMM solution (0.4–0.9 mg/ml, 100–200 μ l) in a 1.5-ml microtube was irradiated with a 100 W mercury lamp (Eikosha, Japan) for 20 min on ice at a distance of about 10 cm through a Pyrex filter as described previously (17, 24). Irradiated samples were analyzed by SDS-PAGE and Western blotting.

Thiophosphorylation—Labeled RLC and HMM were thiophosphorylated with MLCK as described previously (16, 17). Complete thiophosphorylation was verified by urea/glycerol gel electrophoresis (25).

ATPase Assay—Actin-activated MgATPase activity was measured under the following conditions: 0.1 mg/ml HMM, 10 mM MOPS (pH 7.5), 1 mM MgCl₂, 0.1 mM EGTA, 1 mM DTT, 1 mM ATP, and 40 μ M actin at 25°C. The activity was measured by determining the released inorganic phosphate colorimetrically (26).

Gel Electrophoresis and Western Blotting—SDS-PAGE was carried out on a slab gel of 10% acrylamide (0.1% bisacrylamide) according to Porzio and Pearson (27). Separated proteins were transferred to Immobilon-P membrane with a semi-dry system at 0.8 mA/cm² for 1 h according to the manufacturer's instructions (Millipore). To fix proteins on the membrane, the blot was rinsed in water briefly and incubated in 0.05% glutaraldehyde in PBS for 30 min before immunodetection. RLC was detected with rabbit polyclonal anti-RLC antibody (Santa Cruz Biotechnology) and goat anti-rabbit IgG antibody labeled with alkaline phosphatase (Bio Rad) as the first and the second antibodies, respectively.

Amino Acid Sequencing of Cross-Linked Protein—0P-HMM with BP-RLC was irradiated in the presence of 2 mM MgCl₂ and the sample was subjected to SDS-PAGE. Separated protein bands on SDS gel were blotted onto Immobilon-P membrane and stained with Coomassie Brilliant Blue R250. The N-terminal amino acid sequence of the cross-linked product was analyzed by Edman sequencing with Procise 491 cLC (Applied Biosystems).

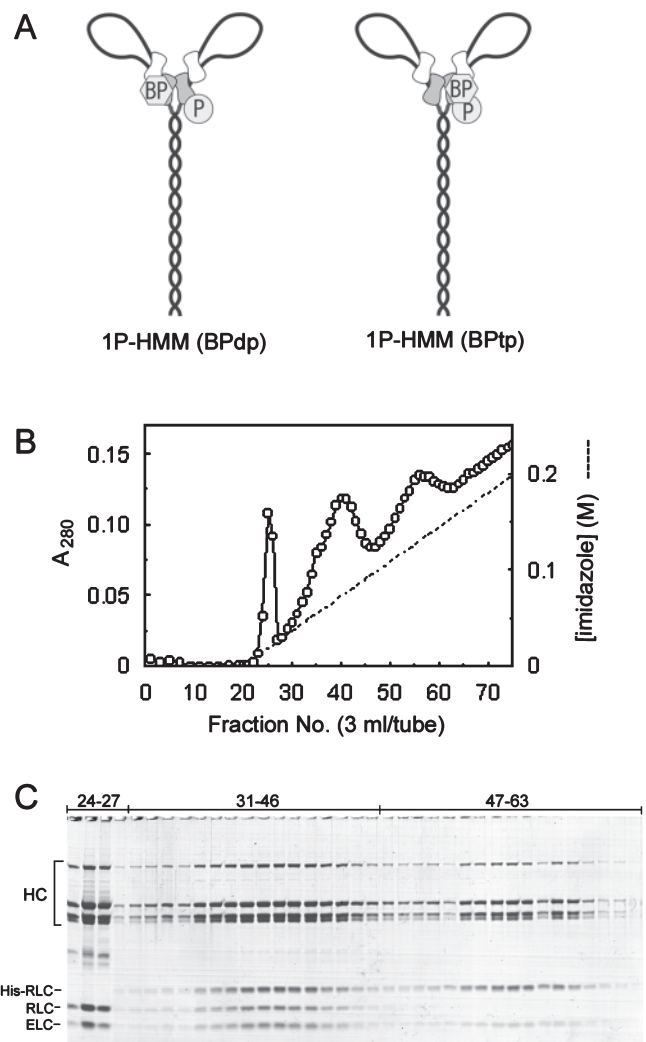


Fig. 1. **Preparation of 1P-HMM.** (A) Two forms of 1P-HMM used in this study are shown schematically. 1P-HMM (BPdp) consists of one native thiophosphorylated RLC and one BP-labeled dephosphorylated RLC. 1P-HMM (BPtp) has one native dephosphorylated RLC and one BP-labeled thiophosphorylated RLC. ELC and RLC in the neck region are shown with open and dark symbols, respectively. BP and P on the RLC indicate the benzophenone label and thiophosphorylation, respectively. (B) Partially exchanged HMM (HMM/thiophosphorylated BP-RLC) was subjected to Ni²⁺-affinity chromatography, and HMM containing thiophosphorylated BP-RLC was eluted with a linear gradient of imidazole. A similar profile was obtained for HMM exchanged with the dephosphorylated BP-RLC (data not shown). (C) Eluted fractions were analyzed by SDS-PAGE. Proteins were stained with Coomassie Brilliant Blue G250. The first peak fractions (24–27) contained nonspecifically bound HMM without His-RLC. The second (31–46) and third (47–63) peak fractions contained the singly and doubly exchanged HMM, respectively.

RESULTS

Preparation of BP-Labeled HMM—To investigate the structural properties of the 1P-HMM, a series of BP-labeled HMMs in various phosphorylated states were prepared (Table 1). The BP moiety was introduced into Cys108 on RLC, which is the only endogenous cysteine in chicken gizzard smooth muscle myosin RLC. Previous

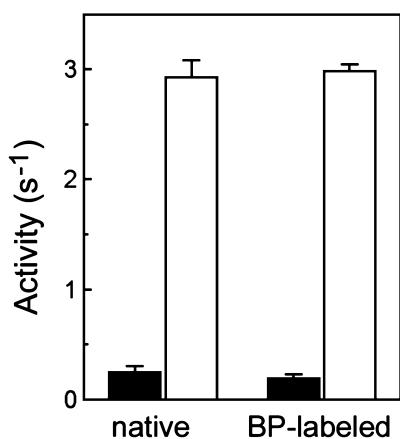


Fig. 2. Actin-activated MgATPase activity. Steady state ATPase activities of native HMM and HMM containing BP-RLC were measured as described in “MATERIALS AND METHODS.” Thiophosphorylated HMM (open bars) was prepared by thiophosphorylation of dephosphorylated HMM (closed bars) with MLCK. The ATPase activities were calculated using a molecular weight of 334,000 for HMM. Averages of measurements for two independent preparations and their standard deviations are shown.

reports demonstrated that introduction of chemical probes at Cys108 had little effect on regulatory properties of smooth muscle myosin (23, 28) and HMM (17, 29), suggesting that the introduction of the BP moiety would have little effect on the structural nature of HMM. Two forms of BP-labeled 1P-HMM (Fig. 1A) were purified by Ni²⁺-affinity chromatography with the aid of a His-tag on the recombinant RLC. The trapped HMMs on Ni²⁺-resin were separated in three peaks by elution with a gentle gradient of imidazole (Fig. 1B). SDS-PAGE analysis (Fig. 1C) showed that nonspecifically bound HMM, without any His-RLC, was eluted in the first peak. HMM containing one His-RLC (*i.e.*, 1P-HMM) was in the second peak, and HMM containing two His-RLCs was in the third peak. To isolate each form of HMM, adequately separated HMM fractions were pooled and concentrated. The His-tag of RLC in the purified HMM was removed by thrombin cleavage to avoid potential effects on the kinetic properties of HMM. However, a 13-amino acid extension (GSGMKETAAAKFE) still remained and caused different migration from native RLC on SDS gel (Figs. 3 and 4).

Dephosphorylated and fully thiophosphorylated HMM with BP-labels were prepared in two ways to examine the potential effects of preparation procedure: (i) endogenous RLC in 0P-HMM was exchanged with the BP-labeled dephosphorylated RLC to yield dephosphorylated BP-HMM, and this was thiophosphorylated with MLCK to yield fully thiophosphorylated BP-HMM (Table 1). (ii) In the affinity chromatography for purification of 1P-HMMs, the third peak fraction was collected as doubly exchanged 0P- or 2P-HMM (Table 1, and Fig. 1, B and C). In the latter procedure, HMM was exposed to non-reducing conditions throughout the series of chromatographies to avoid reduction of Ni²⁺.

Regulation of Labeled HMM—Effects of the exchange procedures and introduction of BP-labeled RLC into HMM were evaluated by ATPase assay. HMM containing

BP-RLC was thiophosphorylated, and activation of the steady-state actin-activated MgATPase activity was examined (Fig. 2). The activity of the BP-HMM was increased more than tenfold by thiophosphorylation, and the results showed phosphorylation-dependent regulation comparable to that of the native HMM. This suggests that HMM containing BP-RLC retains the regulatory properties of the native HMM, consistent with a previous report (17). Furthermore, the steady-state actin-activated MgATPase activities of the BP-labeled 1P-HMMs were approximately half of those of the His-tag purified 2P-HMM containing two BP-RLCs and the native 2P-HMM (data not shown). These measurements are also consistent with a previous report (16), suggesting that the introduction of BP-RLC with the 13-amino acid extension at the N-terminus and the use of non-reducing conditions in the purification procedure have little effect on the phosphorylation-dependent regulation.

Photocross-Linking—HMMs with the BP-RLC were irradiated, and the cross-linked products were analyzed by SDS-PAGE and Western blotting with anti-RLC antibody (Figs. 3 and 4). Irradiation of the 0P- and the 2P-HMM showed different cross-linking reactivities. 0P-HMM (Fig. 3A, lanes 3–5) showed two major cross-linked products at approximately 40 and 90 kDa, whereas only the 40-kDa product was detected in 2P-HMM (lanes 6–8). The cross-linked 40-kDa product was generated under all irradiation conditions and presumed to be an RLC-RLC dimer from its size, as identified previously (17, 29). The product of approximately 90 kDa is novel. It was generated under the low-salt conditions (lane 3) and supposed to be a cross-linked product of the RLC and a heavy chain fragment. The formation of this 90-kDa product was blocked at higher salt concentration (lanes 4 and 5).

The effects of nucleotides and actin on the cross-linkings were examined (Fig. 3B). With 0P-HMM, the amount of the 90-kDa product increased upon addition of MgCl₂ (lane 2), whereas the 90-kDa band disappeared in the presence of ATP (lane 3) and ADP (lane 4). With 2P-HMM (lanes 8–14), the 90-kDa product was not detected under any irradiation conditions. In contrast, little effect was observed on the formation of the 40-kDa product.

In the presence of actin (lane 5), the 90-kDa product was formed in 0P-HMM, but in lower amount than in the absence of actin (lane 2). As in the absence of actin, formation of the 90-kDa product was blocked by addition of nucleotides (lanes 6 and 7); and it was also blocked by thiophosphorylation in the presence of actin (lanes 12–14).

The same cross-linkings and effects of salt concentration and nucleotides were observed with the doubly exchanged 0P- and 2P-HMM, which were purified by Ni²⁺-affinity chromatography in the third peak fractions (data not shown). These results further confirm that the affinity purification procedure has little effect on the structural properties of the BP-HMM, and that the procedure can be applied to the preparation of 1P-HMMs.

The forms of 1P-HMM showed different cross-linking reactivities (Fig. 4). 1P-HMM with the dephosphorylated BP-RLC yielded both the 90- and 40-kDa cross-linked products (Fig. 4A, lane 1), as did 0P-HMM (Fig. 3), while 1P-HMM with the thiophosphorylated BP-RLC formed only the 40-kDa cross-linked product (Fig. 4A, lanes 4–6), like 2P-HMM (Fig. 3). These results clearly indicate that

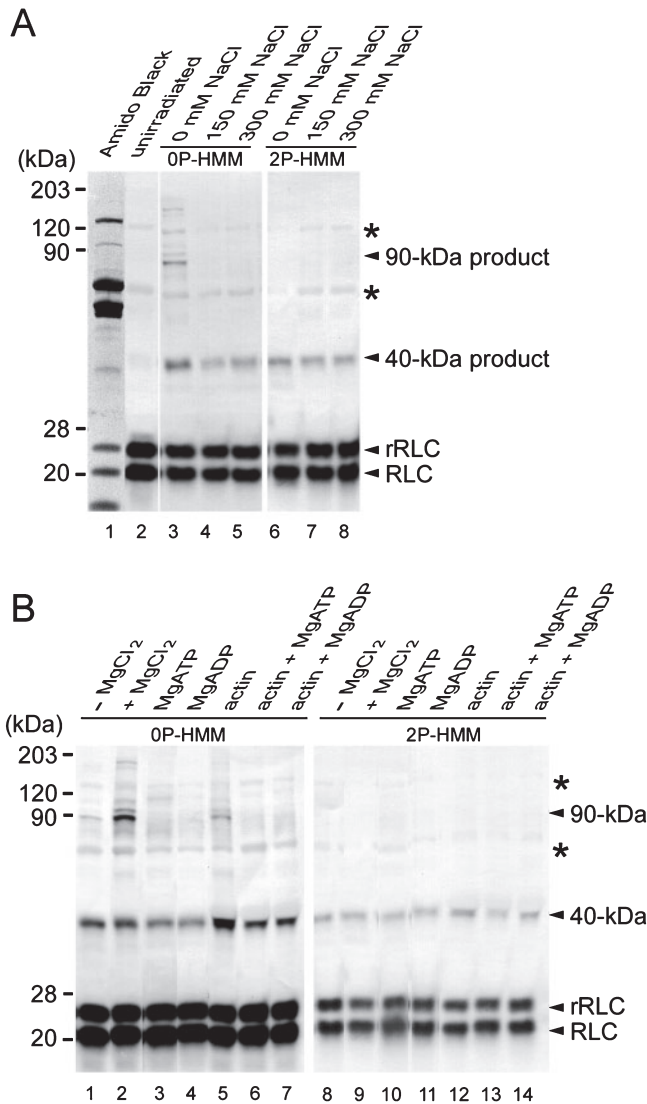


Fig. 3. Photocross-linking in OP- and 2P-HMM. Cross-linked products were detected by Western blotting with anti-RLC antibody for OP- and 2P-HMM. BP-HMM in irradiation buffer [10 mM MOPS (pH 7.5), 0.1 mM EGTA, 2 mM MgCl₂ and 1 mM DTT] was irradiated with additions indicated at the top of the panels. (A) BP-labeled OP- (lanes 3–5) and 2P-HMM (lanes 6–8) were irradiated under various salt conditions. Lane 1, control HMM stained with Amido Black; lane 2, unirradiated control; lanes 3 and 6, HMM without additions. NaCl concentration was 150 mM (lanes 4 and 7) and 300 mM (lanes 5 and 8). A cross-linked product of approximately 40 kDa was detected under all conditions, whereas a product of 90 kDa was detected only under the low salt conditions in OP-HMM (lane 3). (B) Effects of nucleotides and actin on cross-linkings were examined in OP- (lanes 1–7) and 2P-HMM (lanes 8–14). BP-HMM was irradiated in the absence (lanes 1 and 8) and presence (lanes 2–7, and 9–14) of MgCl₂. Additions were as follows: 2 mM MgATP (lanes 3, 6, 10 and 13), 2 mM MgADP (lanes 4, 7, 11 and 14) and 10 μM actin (lanes 5–7 and 12–14). Although the cross-linked products were detected after 5 min of irradiation (data not shown), all samples were irradiated for 20 min to confirm the cross-linking reactivities. The 40-kDa product was detected under all conditions, whereas the 90-kDa product was detected only in the absence of nucleotides in OP-HMM. Asterisks indicate nonspecific bands, which were detected even in the controls (A, lane 2). Positions of size markers are indicated in the left margin.

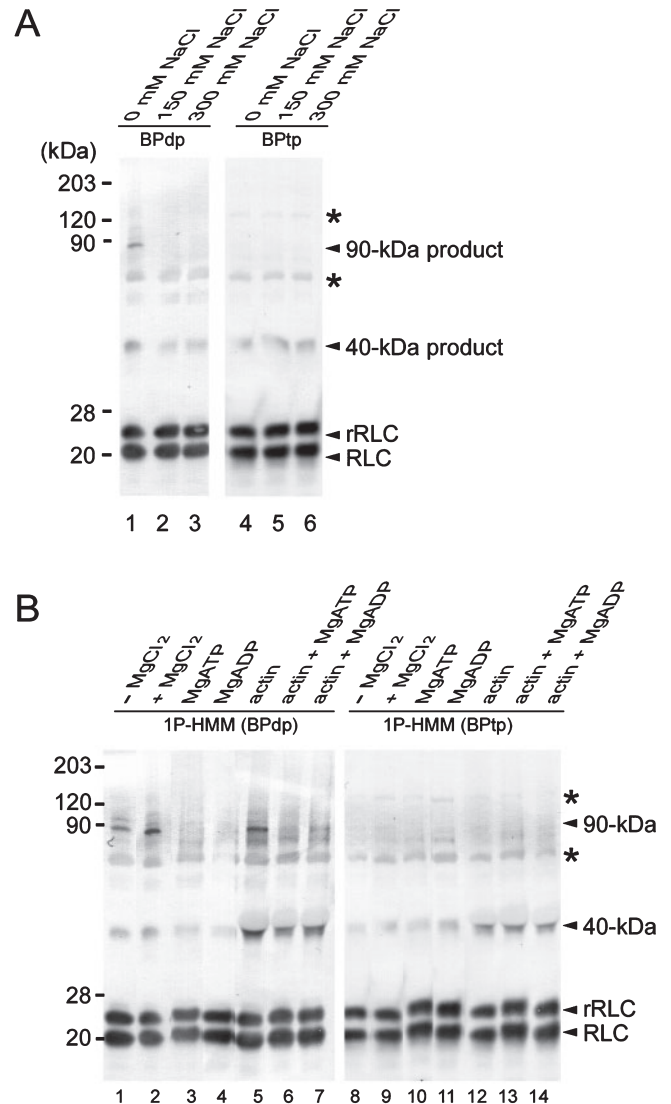


Fig. 4. Photocross-linking in 1P-HMM. BP-HMM in irradiation buffer [10 mM MOPS (pH 7.5), 0.1 mM EGTA, 2 mM MgCl₂ and 1 mM DTT] was irradiated with additions indicated at the top of the panels. (A) 1P-HMM containing the dephosphorylated BP-RLC (lanes 1–3) or the thiophosphorylated BP-RLC (lanes 4–6) was irradiated under various salt conditions. Lanes 1 and 4, HMM without additions. NaCl concentration was 150 mM (lanes 2 and 5) and 300 mM (lanes 3 and 6). A cross-linked product of approximately 40 kDa was detected under all conditions, whereas a product of 90 kDa was detected only under the low salt conditions with 1P-HMM (BPdp) (lane 1). (B) Effects of nucleotides and actin on cross-linkings were examined with 1P-HMM (BPdp) (lanes 1–7) and 1P-HMM (BPtp) (lanes 8–14). BP-HMM was irradiated in the absence (lanes 1 and 8) and presence (lanes 2–7, and 9–14) of MgCl₂. Additions were as follows: 2 mM MgATP (lanes 3, 6, 10 and 13), 2 mM MgADP (lanes 4, 7, 11 and 14) and 10 μM actin (lanes 5–7 and 12–14). The 40-kDa product was detected under all conditions, whereas the 90-kDa product was detected only in the absence of nucleotides with 1P-HMM (BPdp). Asterisks indicate nonspecifically detected bands. Positions of size markers are indicated in the left margin.

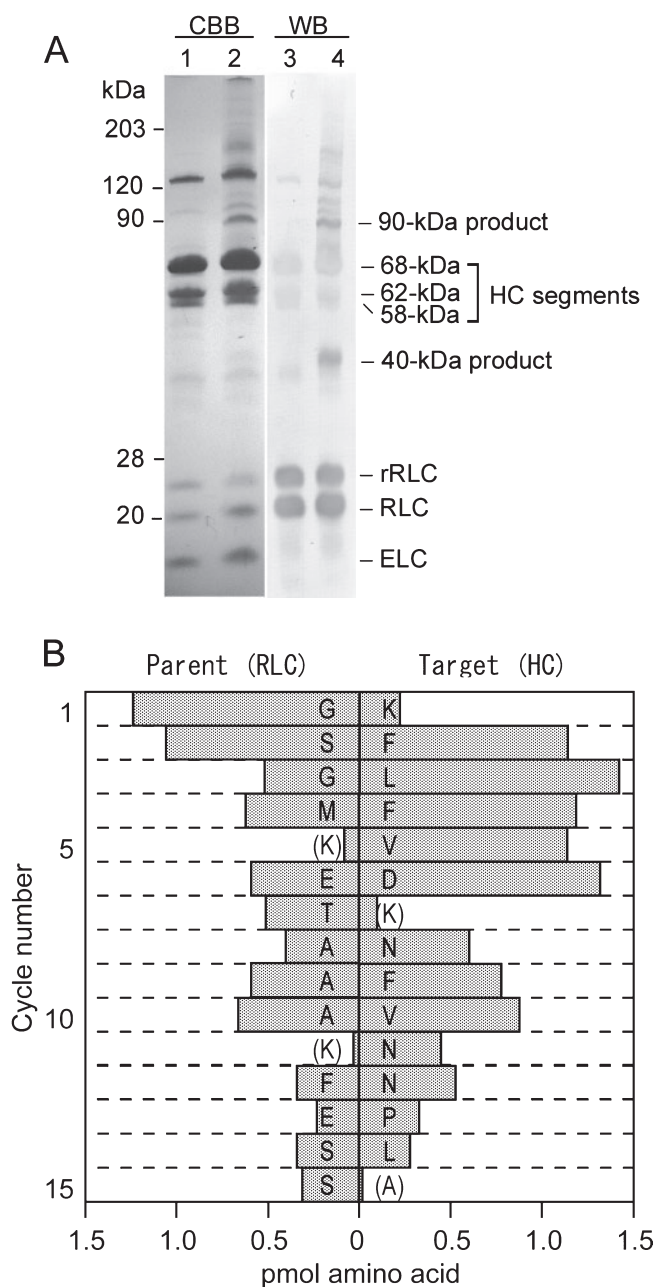


Fig. 5. Amino acid sequencing of the 90-kDa cross-linked product. (A) Unirradiated control (lanes 1 and 3) and irradiated sample (lanes 2 and 4) were separated on SDS gel and transferred to Immobilon-P membrane. The blot was stained with CBB (lanes 1 and 2) and the cross-linked products were detected with anti-RLC antibody (lanes 3 and 4). (B) A single band at 90 kDa, generated by irradiation, was subjected to Edman sequencing. Two major peaks of PTH-amino acids were predominantly detected in each cycle. Single letter codes for amino acid residues without and with parentheses indicate unambiguous and ambiguous assignment, respectively.

each head of 1P-HMM has a different cross-linking reactivity and thus a different structural property. The formation of the 90-kDa product from 1P-HMM was blocked by addition of either salt (Fig. 4A) or nucleotides (Fig. 4B), as in the case of 0P-HMM (Fig. 3).

Identification of the Cross-Linked Region—To identify the possible cross-linked sites in the heavy chain, the

Table 2. Photocross-linking reactivity.

| Phosphorylation states | RLC-RLC (40 kDa) | RLC-HC (90 kDa) |
|------------------------|------------------|-----------------|
| 0P-HMM | + | + ^a |
| 1P-HMM (BPdp) | + | + ^a |
| 1P-HMM (BPtp) | + | – |
| 2P-HMM | + | – |

^aCross-linking was detected only under the low salt conditions.

amino acid sequence of the 90-kDa cross-linked product was analyzed (Fig. 5). Since the presence of MgCl₂ increased the formation of the 90-kDa product (Fig. 3B), the 0P-HMM was irradiated in the presence of 2 mM MgCl₂ and subjected to SDS-PAGE (Fig. 5A). The 90-kDa product on SDS gel was transferred onto Immobilon-P membrane for direct sequencing. Two major peaks were obtained in each Edman degradation cycle and two independent sequences were identified: GSGMKETAAAK-FES¹S² and K¹⁰FLFVDKNFVNPLA²⁴ (Fig. 5B). The former is the N-terminal sequence of the recombinant RLC containing a 13-amino acid extension, and the latter corresponds to that of the N-terminal 68-kDa heavy chain segment produced by the V8 protease digestion (8).

DISCUSSION

Photocross-Linking Reactivity—Examining biochemical properties of the singly phosphorylated myosin is expected to provide useful information about the phosphorylation-dependent regulatory mechanism of smooth muscle myosin. In this study, we investigated structural properties of the singly phosphorylated HMM using a photocross-linking technique. We prepared a series of photoreactive HMMs containing BP-labeled RLC in various phosphorylation states and examined their cross-linking reactivities (Table 2). Two major cross-linked products with apparent molecular mass of 90 and 40 kDa were detected in the dephosphorylated state, whereas only the 40-kDa product was detected in the fully phosphorylated state. The 90-kDa product was a result of cross-linking between the RLC and the N-terminal 68-kDa segment of the heavy chain (Fig. 5). These results indicate that the phosphorylation alters the spatial relationship between the RLC and the heavy chain, and that the BP moiety at Cys108 can be a sensor for this alteration, which allows us to distinguish the structural properties of HMM in various phosphorylation states.

In the singly phosphorylated state, the two heads had different cross-linking reactivities (Table 2). This result indicates that two heads in the singly phosphorylated state can take an asymmetric orientation and that the structure of 1P-HMM is different from those of 0P- and 2P-HMM. Therefore, it is likely that phosphorylation of one of the two heads can result in a functional alteration, that is, the ATPase and motor activities that are characteristic of 1P-HMM (discussed below).

Cross-Linking between the RLC and the Heavy Chain—The 90-kDa product was a result of the cross-linking to the 68-kDa segment of the motor domain, not to the light chain-binding domain, where BP-RLC binds directly. The crystal structure of nucleotide-free S1 shows that Cys108 on the RLC is positioned far from the 68-kDa segment

(straight conformation) and out of range of the cross-linking (30). Thus, cross-linking between the RLC and the 68-kDa segment requires large motions in the head domains, that is, a flexible motion around the head-rod junction and/or a large rotation in a single head domain, especially in the lever arm. A flexible motion around the head-rod junction will allow cross-linking in the inter-head domains, and a large rotation in the lever arm will allow cross-linking in an intra-head domain. It is, however, uncertain whether the cross-linking involves intra-head or inter-head domains. The straight conformation observed in the crystal structure of S1 (30) was also found in the nucleotide-free smooth muscle S1 in solution (31). These observations suggest that a large rotation in the lever arm, which would allow Cys108 to approach the 68-kDa segment of its own head, is less likely to occur in the absence of nucleotide.

The amount of the 90-kDa cross-linking increased in the presence of Mg^{2+} (Figs. 3B and 4B). Mg^{2+} is bound to the first EF-hand of the RLC (32, 33) and thereby stabilizes the RLC binding to the heavy chain. This stabilization of the RLC may increase the frequency with which the RLC approaches within 1 nm of the 68-kDa segment. At the same time, the cross-linking was decreased by addition of salt, suggesting that the cross-linkable conformation is stabilized by weak ionic interaction under low salt conditions.

Addition of nucleotides substantially diminished the formation of the 90-kDa product (Figs. 3 and 4). ATP stabilizes the flexed conformation of both the dephosphorylated and the phosphorylated HMM under low salt conditions, where the two heads bend back toward the tail (34). If the flexed conformation was involved in the formation of the 90-kDa product, the presence of ATP would increase the amount of the 90-kDa product. In the present study, however, the 90-kDa product disappeared upon addition of ATP, suggesting that the flexed conformation may not be involved in the cross-linking. In addition, the 10S myosin exchanged with BPdp-RLC formed cross-links to a portion of LMM, but not to the 68-kDa segment (23).

Phosphorylation-Dependent Cross-Linking—Cross-linking between the RLC and the heavy chain was substantially blocked by phosphorylation. Three possible explanations were considered, as follows. (i) Phosphorylation may limit the motion of the head domains, resulting in inhibition of the cross-linking in the inter-head domains. Considering that benzophenone can trap a target rapidly, even though the target is a transient one (35), the phosphorylation of one head may restrict approach of the partner head to within 1 nm from Cys108 on the phosphorylated RLC. Sheng *et al.* showed that the two heads in the dephosphorylated myosin were distributed equally in separated and closely apposed conformations, whereas the thiophosphorylated myosin favored the separated conformation (36). This observation suggests that the phosphorylated heads are somewhat restricted in their motion, leading to separation of the two heads. (ii) Phosphorylation may limit rotation in the lever arm, resulting in inhibition of the cross-linking in an intra-head domain. If the phosphorylated RLC stabilizes the lever arm and thereby limits rotation in the lever arm, Cys108 of the RLC will not be able to approach the 68-kDa seg-

ment of its own head. However, the distance between Cys108 and the 68-kDa segment in S1 was not affected by phosphorylation (31), suggesting that the phosphorylation could not alter the cross-linking reactivity by stabilizing the lever arm. (iii) The phosphorylation may change the conformation of the RLC and thereby result in shielding of the BP moiety from the 68-kDa segment. Wu *et al.* demonstrated that the spatial relationship between the N- and the C-termini of the RLC was altered by phosphorylation (37). This alteration may result in the shielding of the BP moiety and thereby inhibit the cross-linking. In this interpretation, both the intra-head and inter-head cross-linking between RLC and heavy chain could be inhibited by phosphorylation. Further study is required to elucidate whether the blocking of the cross-linking is due to the alteration in the spatial relationship of the two heads or to the conformational change of the RLC.

Formation of the RLC-RLC dimer was detected regardless of the phosphorylation state in this study, but was stated to be blocked by phosphorylation in an earlier report (17), which led the authors to propose a phosphorylation-dependent regulatory mechanism. Considering that the cross-linked region was located in the flexible N-terminal region (R4–R16) (29), these conflicting results can arise from the difference in the N-terminal extra residues, that is, the 13-amino acid extension in our recombinant RLC compared with 4-amino acid extension in the previous study (17). Therefore, even though the phosphorylation can remove the N-terminus of the RLC from Cys108 on the partner RLC, the additional 9 more residues may allow it to access the range of the RLC-RLC cross-linking.

Our finding of the phosphorylation-dependent cross-linking between RLC and heavy chain indicates that Cys108 of the RLC is close to the 68-kDa segment, and that phosphorylation induces a conformational change that keeps Cys108 away from the segment as well as the N-terminus of the partner RLC (29). Considering that the phosphorylation-dependent release from the inhibitory interactions of the dephosphorylated HMM should involve structural change in the head domains, the phosphorylation-dependent conformational change demonstrated here can work as a part of structural basis for the phosphorylation-dependent regulation.

Asymmetric Property of 1P-HMM—As demonstrated in the present work, each head of 1P-HMM has asymmetric cross-linking reactivities. These results clearly indicate that the structural properties of the two heads in 1P-HMM are different from those of the 0P- and the 2P-HMM, suggesting that the single phosphorylation can alter the enzymatic properties of HMM. If the cross-linking of the RLC and the heavy chain was formed in an intra-head domain, the blockage by phosphorylation of the cross-linking in 1P-HMM (BPtp) could be construed as being the result of an independent structural alteration of the head by phosphorylation. In this interpretation, structural alteration in the phosphorylated head could result in an independent activation of the head, as suggested by Harris *et al.* (15). On the other hand, if the cross-linking was formed in the inter-head domains, blocking by phosphorylation could be construed as being the result of a cooperative alteration in the orientation of

the two heads. Wendt *et al.* proposed an inhibitory interaction model, in which the motor domain of one head was positioned in proximity to the partner regulatory domain (38). Considering their inhibitory model and the cooperative alteration presented above, one of the heads in 1P-HMM could still approach the partner head's regulatory domain and thus be in an inhibitory conformation, whereas the other head could not approach the partner head. In this assumption, the probability of HMM being in an inhibitory conformation could be decreased by single phosphorylation and thus result in a partial and cooperative activation of both heads as demonstrated by Ellison *et al.* (16). However, the phosphorylation-dependent cooperative change in the structural properties was not established in the present study, since it is uncertain whether the cross-linking between the RLC and the heavy chain involved intra-head or inter-head domains. Further study is required to establish the effects of single phosphorylation on the activity of both heads. It also remains to be solved whether each head of 1P-HMM has an asymmetric property under physiological ionic conditions.

We thank Dr. H. Kawai (Division of Chemistry, Graduate School of Science, Hokkaido University) for his help in the cross-linking experiments. We are also grateful to Mr. T. Hirose (Center for Instrumental Analysis, Hokkaido University) for technical assistance in peptide sequencing.

REFERENCES

- Sellers, J.R., Eisenberg, E., and Adelstein, R.S. (1982) The binding of smooth muscle heavy meromyosin to actin in the presence of ATP. Effect of phosphorylation. *J. Biol. Chem.* **257**, 13880–13883
- Sellers, J.R. (1985) Mechanism of the phosphorylation-dependent regulation of smooth muscle heavy meromyosin. *J. Biol. Chem.* **260**, 15815–15819
- Trybus, K.M. (1989) Filamentous smooth muscle myosin is regulated by phosphorylation. *J. Cell Biol.* **109**, 2887–2894
- Warshaw, D.M., Desrosiers, J.M., Work, S.S., and Trybus, K.M. (1990) Smooth muscle myosin cross-bridge interactions modulate actin filament sliding velocity *in vitro*. *J. Cell Biol.* **111**, 453–463
- Trybus, K.M. (1994) Regulation of expressed truncated smooth muscle myosins. Role of the essential light chain and tail length. *J. Biol. Chem.* **269**, 20819–20822
- Katoh, T. and Morita, F. (1996) Roles of light chains in the activity and conformation of smooth muscle myosin. *J. Biol. Chem.* **271**, 9992–9996
- Seidel, J.C. (1980) Fragmentation of gizzard myosin by α -chymotrypsin and papain, the effects on ATPase activity, and the interaction with actin. *J. Biol. Chem.* **255**, 4355–4361
- Ikebe, M. and Hartshorne, D.J. (1985) Proteolysis of smooth muscle myosin by *Staphylococcus aureus* protease: preparation of heavy meromyosin and subfragment 1 with intact 20 000-dalton light chains. *Biochemistry* **24**, 2380–2387
- Sata, M., Matsuura, M., and Ikebe, M. (1996) Characterization of the motor and enzymatic properties of smooth muscle long S1 and short HMM: role of the two-headed structure on the activity and regulation of the myosin motor. *Biochemistry* **35**, 11113–11118
- Cremona, C.R., Sellers, J.R., and Facemyer, K.C. (1995) Two heads are required for phosphorylation-dependent regulation of smooth muscle myosin. *J. Biol. Chem.* **270**, 2171–2175
- Konishi, K., Katoh, T., Morita, F., and Yazawa, M. (1998) Conformation, filament assembly, and activity of single-headed smooth muscle myosin. *J. Biochem.* **124**, 163–170
- Sweeney, H.L., Chen, L.Q., and Trybus, K.M. (2000) Regulation of asymmetric smooth muscle myosin II molecules. *J. Biol. Chem.* **275**, 41273–41277
- Konishi, K., Katoh, T., Yazawa, M., Kato, K., Fujiwara, K., and Onishi, H. (2001) Two new modes of smooth muscle myosin regulation by the interaction between the two regulatory light chains, and by the S2 domain. *J. Biochem.* **129**, 365–372
- Cremona, C.R., Wang, F., Facemyer, K., and Sellers, J.R. (2001) Phosphorylation-dependent regulation is absent in a nonmuscle heavy meromyosin construct with one complete head and one head lacking the motor domain. *J. Biol. Chem.* **276**, 41465–41472
- Harris, D.E., Stromski, C.J., Hayes, E., and Warshaw, D.M. (1995) Thiophosphorylation independently activates each head of smooth muscle myosin *in vitro*. *Amer. J. Physiol.* **269**, C1160–1166
- Ellison, P.A., Sellers, J.R., and Cremona, C.R. (2000) Kinetics of smooth muscle heavy meromyosin with one thiophosphorylated head. *J. Biol. Chem.* **275**, 15142–15151
- Wu, X., Clack, B.A., Zhi, G., Stull, J.T., and Cremona, C.R. (1999) Phosphorylation-dependent structural changes in the regulatory light chain domain of smooth muscle heavy meromyosin. *J. Biol. Chem.* **274**, 20328–20335
- Yoshida, M. and Yagi, K. (1988) Two kinds of myosin phosphatases with different enzymatic properties from fresh chicken gizzard smooth muscle. Purification and characterization. *J. Biochem.* **103**, 380–385
- Spudich, J.A. and Watt, S. (1971) The regulation of rabbit skeletal muscle contraction. I. Biochemical studies of the interaction of the tropomyosin-troponin complex with actin and the proteolytic fragments of myosin. *J. Biol. Chem.* **246**, 4866–4871
- Yoshida, M. and Yagi, K. (1986) Purification and characterization of a phosphoprotein phosphatase that dephosphorylates myosin and the isolated light chain from chicken gizzard smooth muscle. *J. Biochem.* **99**, 1027–1036
- Yazawa, M., Sakuma, M., and Yagi, K. (1980) Calmodulins from muscles of marine invertebrates, scallop and sea anemone. *J. Biochem.* **87**, 1313–1320
- Gornall, A.G., Bardawill, C.J., and David, M.M. (1949) Determination of serum proteins by means of the biuret reaction. *J. Biol. Chem.* **177**, 751–766
- Olney, J.J., Sellers, J.R., and Cremona, C.R. (1996) Structure and function of the 10 S conformation of smooth muscle myosin. *J. Biol. Chem.* **271**, 20375–20384
- Cremona, C.R., Grammer, J.C., and Yount, R.G. (1991) Vanadate-mediated photocleavage of myosin. *Methods Enzymol.* **196**, 442–449
- Perrie, W.T. and Perry, S.V. (1970) An electrophoretic study of the low-molecular-weight components of myosin. *Biochem. J.* **119**, 31–38
- Trybus, K.M. (2000) Biochemical studies of myosin. *Methods* **22**, 327–335
- Porzio, M.A. and Pearson, A.M. (1977) Improved resolution of myofibrillar proteins with sodium dodecyl sulfate-polyacrylamide gel electrophoresis. *Biochim. Biophys. Acta* **490**, 27–34
- Morita, J., Takashi, R., and Ikebe, M. (1991) Exchange of the fluorescence-labeled 20 000-dalton light chain of smooth muscle myosin. *Biochemistry* **30**, 9539–9545
- Wahlstrom, J.L., Randall, M.A., Jr., Lawson, J.D., Lyons, D.E., Siems, W.F., Crouch, G.J., Barr, R., Facemyer, K.C., and Cremona, C.R. (2003) Structural model of the regulatory domain of smooth muscle heavy meromyosin. *J. Biol. Chem.* **278**, 5123–5131
- Rayment, I., Rypniewski, W.R., Schmidt-Base, K., Smith, R., Tomchick, D.R., Benning, M.M., Winkelmann, D.A., Wesenberg, G., and Holden, H.M. (1993) Three-dimensional structure of myosin subfragment-1: a molecular motor. *Science* **261**, 50–58
- Xiao, M., Reifenberger, J.G., Wells, A.L., Baldacchino, C., Chen, L.Q., Ge, P., Sweeney, H.L., and Selvin, P.R. (2003) An actin-dependent conformational change in myosin. *Nat. Struct. Biol.* **10**, 402–408

32. Messer, N.G. and Kendrick-Jones, J. (1988) Molecular cloning and sequencing of the chicken smooth muscle myosin regulatory light chain. *FEBS Lett.* **234**, 49–52
33. da Silva, A.C., Kendrick-Jones, J., and Reinach, F.C. (1995) Determinants of ion specificity on EF-hands sites. Conversion of the $\text{Ca}^{2+}/\text{Mg}^{2+}$ site of smooth muscle myosin regulatory light chain into a Ca^{2+} -specific site. *J. Biol. Chem.* **270**, 6773–6778
34. Suzuki, H., Stafford, W.F., 3rd., Slayter, H.S., and Seidel, J.C. (1985) A conformational transition in gizzard heavy meromyosin involving the head-tail junction, resulting in changes in sedimentation coefficient, ATPase activity, and orientation of heads. *J. Biol. Chem.* **260**, 14810–14817
35. Dorman, G. and Prestwich, G.D. (1994) Benzophenone photophores in biochemistry. *Biochemistry* **33**, 5661–5673
36. Sheng, S., Gao, Y., Khromov, A.S., Somlyo, A.V., Somlyo, A.P., and Shao, Z. (2003) Cryo-atomic force microscopy of unphosphorylated and thiophosphorylated single smooth muscle myosin molecules. *J. Biol. Chem.* **278**, 39892–39896
37. Wu, G., Wong, A., Qian, F., and Lu, R.C. (1998) Phosphorylation changes the spatial relationship between Glu124–Arg143 and Cys18 and Cys165 of the regulatory light chain in smooth muscle myosin. *Biochemistry* **37**, 7676–7685
38. Wendt, T., Taylor, D., Trybus, K.M., and Taylor, K. (2001) Three-dimensional image reconstruction of dephosphorylated smooth muscle heavy meromyosin reveals asymmetry in the interaction between myosin heads and placement of subfragment 2. *Proc. Natl. Acad. Sci. USA* **98**, 4361–4366